Contents lists available at GrowingScience

Current Chemistry Letters

homepage: www.GrowingScience.com

Design and synthesis of potential pyrrole-coupled carboxamide derivatives as an anti-superbug MRSA agent

Boobal Arasu Velu[a], Ganesamoorthy Thirunarayanan[a*] and Sivakumar Kulanthaivel[b]

[a]*Department of chemistry, Annamalai University, Annamalai Nagar-608002, Tamil Nadu, India*
[b]*Department of chemistry, Adhiyamaan College of Engineering, Hosur-635109, Tamil Nadu, India*

C H R O N I C L E

Article history:
Received March 20, 2023
Received in revised form
June 9, 2023
Accepted August 17, 2023
Available online
August 17, 2023

Keywords:
Pyrrole coupled carboxamide derivatives
Molecular docking
Biocompatibility and Toxicity

A B S T R A C T

A series of new pyrrole-coupled carboxamide derivatives had been synthesized and amply characterized by various techniques, viz FTIR, 1H-NMR, 13C-NMR, and LCMS. All these compounds had undergone evaluation for their PASS, BBB, pharmacophore model, ADME, and bioactive score. The antibacterial properties of all the derivatives were examined and compound **5i** demonstrated strong antibacterial activity against MRSA. A membrane damage investigation supported by SEM pictures, cellular content leakage, potassium efflux, and bacterial respiration suppression showed that compound **5i** had anti-MRSA properties. A good binding score of -9.11 was found for compound **5i** against the MRSA protein 6FTB in an in silico molecular docking analysis, compared to a score of -10.25 for streptomycin. Based on these findings, compound **5i** can be further studied in order to develop it as a drug to treat MRSA infections.

1. Introduction

Infections caused by bacterial pathogens pose a constant threat to human health. Because of the rapid development of resistance to conventional drug therapy, the drug resistance of bacteria has become a more serious one[1]. Since ancient times, natural compounds derived from plants, animals, or microbes have been employed to heal pathological disorders[2]. However, due to several causes that have resulted in the re-emergence of these diseases, they continue to be a major and difficult health problem. Antibiotic resistance, population growth, international travel, migration, the rise in the number of immune-compromised patients, and climate change are all important elements in the fight against infectious illnesses[3]. The discovery of molecules with desired physico-chemical, pharmacokinetic, and pharmacodynamics characteristics are a critical issue in medicinal chemistry, and it can be aided by *in silico* research [4]. The pivotal difficulty of drug development is continuous optimization of lead compounds to obtain novel drug-like molecules [5]. Heterocyclic chemistry is a branch of organic chemistry that involves a wide range of pharmacologically active compounds that can be either synthesized in the lab or obtained from nature. Within the cyclic structure, these are the compounds which contain one or more heteroatoms such as oxygen, sulfur, nitrogen, or the mixture of the heteroatoms with at least one carbon [6]. Pyrrole is one of the latest heterocyclic moieties, that has received a lot of attention because of its pharmacological effects. Its abundance in natural goods, pharmaceuticals, and new materials has pushed the chemistry of pyrrole and its derivatives to the forefront of research [7]. Although pyrrole does not occur naturally, numerous of its derivatives can be found in several cofactors and in natural products [8-9]. With a high frequency of good hits in biological screens of this heterocycle and its congeners, piperazine is now the most important building block employed in drug discovery. A review of the literature found that piperazine derivatives are important pharmacophores in a variety of therapeutic domains, acting as antifungal, antibacterial agents[10]. Vitamin B12, bile pigments such as bilirubin and biliverdin, and the porphyrins of heme, chlorophyll, chlorins, bacteriochlorins, and porphyrinogens are all examples of naturally occurring pyrrole-containing compounds. PQQ, makaluvamine M, ryanodine, rhazinilam, lamellarin, prodigiosin, myrmicarin, and sceptrin are examples of pyrrole-

* Corresponding author. Tel.: +91 97010499846
E-mail address drgtnarayanan@gmail.com (G. Thirunarayanan)

doi: 10.5267/j.ccl.2023.8.005

containing secondary metabolites[11-12]. In pharmacologically active drugs, the pyrrole has a variety of biological properties such as antifungal agents, antimicrobial agents, anti-inflammatory agents, HMG-CoA reductase inhibitors, antitumor agents, antidepressants, antivirus agents, anti-tubercular agents, antihypertensive agents, antimalarial agents, antiulcer agents, mGluR1 antagonists, DPP IV inhibitors, insecticidal agents, histone deacetylase inhibitors, cannabinoid receptor antagonists, allosteric receptor antagonist [13].The pyrrole-based carboxamide molecule is a pharmacophore found as a core skeleton in molecules with a variety of biological activities, including insecticidal[14], antibiofilm[15], antibacterial [16], ATPase inhibitors of DNA gyrase [17], DNA binding, topoisomerase inhibition, inducible nitric oxide synthase (nNOS and iNOS) inhibitors[18], antifungal, anticancer, JAK2 inhibitors [19], antitumor [20]. Compounds that have a pyrrole based carboxamide scaffold in their skeleton have a wider range of biological activities [21]. Machine-aided designs are used in medicinal chemistry and biological research to predict the behavior of physiologically active chemicals, which helps in the design of acceptable medication systems. It's simple to figure out which section of the molecule is therapeutically active [22]. In this study, all synthesized compounds were subjected to both *in-vivo* and *In-silico* analysis (ADME, PASS, Bioactivity score, molecular docking) to evaluate whether the compounds have the drug-like property are not.

2. Materials and methods

All chemicals were sourced from Sigma Aldrich, Bangaluru, India. All synthesis were carried out using analytical research grade chemicals and reagents. For column chromatography, used silica gel supplied by Merck Pvt Limited, Mumbai, India. The IR spectra were recorded using an Agilent Cary 630 FTIR spectrometer. Spectra were run in the range of 400-4000 cm^{-1} at room temperature. The ^{1}H and ^{13}C NMR spectra were recorded using a 400 MHz Agilent NMR and $CDCl_3$ was used as solvent. The chemical shifts were reported in parts per million (ppm) relative to TMS. A Waters micro TOF QII mass spectrometer was used for the mass spectroscopic analysis. Microbial Type Culture Collection (MTCC), Chandigarh, India, provided the lyophilized reference *Staphylococcus aureus*-96 and *Staphylococcus epidermidis*- 435 strain, and strains were cultured in recommended broth according to the revival procedure provided by MTCC. The necessary culture medium was purchased from Hi-Media Laboratories, Mumbai, India.

2.1. Synthesis of pyrrole ligands

Compound (Z)-1-(1-methyl-1H-pyrrol-2-yl)-N-(2-(piperazin-1-yl)ethyl)methanimine **(3)** was synthesized by reacting 1-methyl-1H-pyrrole-2-carbaldehyde **(1)** (1 equivalent) with 2-(piperazin-1-yl)ethan-1-amine **(2)** (1 equivalent) . Compounds **(1)** and **(2)** were dissolved in 20 ml of methanol, 2-3 drops of acetic acid were added as a catalyst and refluxed the reaction mixture for 6-8 hrs. Progress and completion of the reaction was monitored using thin layer chromatography (TLC). The obtained product **(3)** (1equivalent) was further refluxed with methanolic solution of substituted isocyanato benzene (1equivalent), in the presence of triethylamine, for about 6-7 hrs. The solid was dried and recrystallized from methanol. A yellowish product was obtained in good yield.

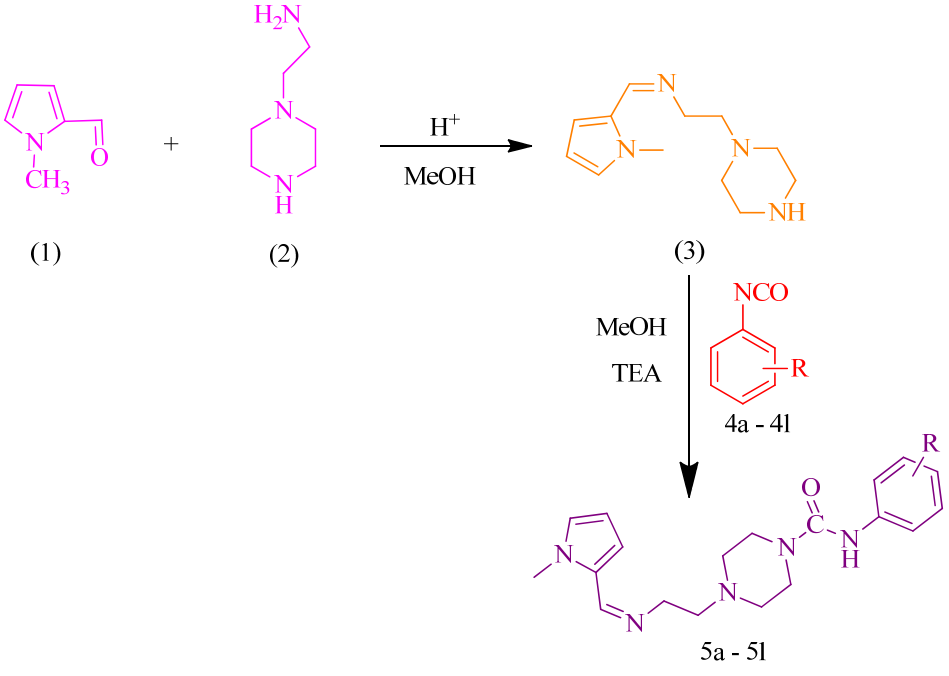

Fig. 1. Scheme for the synthesis of pyrrole derivatives

2.2. ADME- Absorption, Distribution, Metabolism and Excretion analysis and BBB- Blood Brain Barrier Permeability

A molecule's proper absorption, distribution, metabolism, and excretion in the human body decides how effective it is. Numerous major inputs can be gathered, which are helpful for analyzing a molecule's desirable qualities, thanks to the accessibility of a wide range of experimental techniques, such as high throughput in-vitro ADME screens and *in-silico* ADME analysis. Computational ADME should be utilized in conjunction with in-vivo and in-vitro estimations in the early stage of drug development process because it lowers the number of safety concerns. To ascertain crucial pharmacokinetic metrics like ADME, Lipinski's rule must be applied to the molecular characteristics of a drug candidate. We evaluated ADME properties using Mol Inspiration, an online property calculation toolset available at doi: http://www.molinspiration.com[23]. The CB Ligand-BBB prediction database, available at doi: http://www.cbligand.org.

2.3. Prediction of Activity Spectra for test Substances

The PASS (Prediction of Activity Spectra for Substances) technique is used for statistical screening of potential biological effects, such as antihistaminic effect[24] and associated behaviors such as anti-allergic and anti-asthmatic effect[25], histamine release inhibition, rhinitis treatment, immunomodulation, bronchodilation, antilog activities, anti-IL activity, PDE inhibition, anti-5HT3 activity, and so on. The total biological potential of an organic drug-like candidate is determined with the help of this software. PASS represents a variety of biological activities in real time using the structure of organic molecules. PASS can be used to assess the biological activity profiles of virtual molecules before chemical synthesis and biological investigation. It forecasts the desired pharmacological effect, the molecular mechanisms of action, and the likelihood of undesirable side effects such mutagenicity, teratogenicity, carcinogenicity, and embryotoxicity[26]. This method also gives quantitative structure-activity relationships by examining chemical structures with 2D and/or 3D descriptors and then using bioactive ligands to develop models. Constructing models with bioactive ligands after analysing chemical substances with 2D and/or 3D descriptors. Using this approach, the authors were able to establish quantitative structure-activity relationship. Additionally, the calculated values of Pi (probably inactivity) and Pa (probable activity) were used to assess the synthesized molecule's activity. For a particular biological activity, compounds having a Pa value greater than Pi were taken into consideration.

2.4. Molecular docking Study

In the current investigation, lipid II-bound MRSA glycosyltransferase protein like 6FTB (PDB id) was targeted using the synthesized compounds, the pyrrole-based carboxamide analogues 5(a-l). The formation of bacterial cell wall depends on this lipid(6FTB). The experimental results clearly showed that the pyrrole-based carboxamide analogues 5(a-l) had an inhibitory effect on MRSA growth in *in-vitro* antibacterial investigation. The *in-silico* molecular docking method was used to provide a more scientific means of validating the compound's interaction with target protein of pathogenic superbug MRSA. Protein 6FTB from the RCSB Protein Data Bank was used to execute molecular docking in order to assess the behavior of *S.aureus* at biological interfaces. Using Autodock 1.5.7 software's protein preparation procedure, which incorporates energy minimization, the crystal structure was refined or synthesized in a multistep process. Using the OPLS-2005 force field, the right bond ordering was ascribed, hydrogen atoms were introduced, and water molecules beyond 5Å from the hetero atom were deleted. Formal charges, and amide groups of Asn and Gln were optimized. All amino acid flips were allocated to address geometry, and hydrogen bonds were reinforced. With the use of PROPKA, the pH was adjusted to 7.5. Non-hydrogen atoms were reduced to a default RMSD of 0.3 using the controlled reduction method. Extra-accuracy (XP) docking and scoring were used to dock each molecule into the receptor grid of radii 30Å x 30Å x 30Å and the docking computation was rated based on the Glide score[27].

2.5. Antibacterial studies MRSA

2.5.1. Preparation of bacterial culture

The single purified colony was taken from the frozen glass beads of glycerol vial stock (previously culture coated on glass beads and stored at -18 to -22° C). The glass bead was incubated in Brain heart infusion (BHI) broth for 24 hours at 37° C. Using UV-vis spectroscopy at 600 nm, cell density was adjusted to $1x10^6$ CFU/mL.

2.5.2. Minimum inhibitory concentration by resazurin assay

The MIC value of the synthesized analogues were determined by dispensing sterile BHI broth into each of 96 wells and mixing different concentrations of synthesized analogues dissolved in dimethyl sulfoxide (DMSO) with fluid BHI broth. Added 10 µL of resazurin indicator solution (270 mg resazurin in 40 mL sterilized distilled water) in each well. After that, 10 µL of bacterial suspension ($5x10^6$ CFU/mL) was added to yield $5x10^5$ CFU/mL. From the list of broad-spectrum antibiotics, streptomycin was used as standard bactericidal agents. As a positive control, a combination of all additions except the test compound was used. Negative controls included all solutions without the addition of bacterial culture. After wrapping the plates in thin plastic films, they were incubated at 37° C for 24 hours[28].

2.5.3 Disc diffusion method

The synthesized analogues were tested for antibacterial activity in a dose-dependent manner using the disc diffusion method. The overnight culture was used to prepare the bacterial culture, and 1×10^7 CFU/mL cells were inoculated onto nutrient agar, followed by the placement of a sterile disc (6 mm) loaded with different concentrations of synthesized derivatives on the agar. The positive control was streptomycin (10µg/disc), and the negative control was sterile saline water. The plates were inverted and incubated at 37° C for 24 hours to examine the zone of inhibition (ZOI)[29].

2.6 Study of MRSA cell membrane damage

The MRSA cell suspension was treated with the minimum inhibitory concentration (MIC) of compound **5i** for up to 2 hrs. The control and treated cells were mixed in PBS with 2.5% glutaraldehyde and deposited on a glass slide after being treated with 30-100% ethanol separately. The cells were allowed to dry at room temperature for two days before examining them in a SEM to study the cell damage as described.

2.6.1 Release of cellular material

The cellular material (DNA leakage) was measured using Chauhan and Kang's method. MRSA cell culture was treated with compound **5i** at its MIC value and incubated at 37° C for 0, 30, 60, 90, 120, and 150 minutes before being pelletized by centrifugation at 3500 rpm and the OD of the supernatant at 260 nm was measured in a spectrophotometer. All assays were carried out in triplicate.

2.6.2 Evaluation of MRSA cell damage by potassium efflux

Wang's method was used to assess MRSA cell membrane damage by measuring the difference in potassium efflux. The culture was pelletized and re-suspended in 100 mM sodium phosphate buffer (pH 7). MRSA cell density was adjusted to OD of 0.7 at 600 nm. In a 100 mL beaker, MRSA cell suspension was treated with double the MIC of compound **5i** and magnetically stirred at 37° C. The MRSA cell suspension was withdrawn at regular intervals of 0, 30, 60, 90, 120, and 150 minutes, and the intensity of the supernatant was measured at 766.5 nm using ICP-OES (PerkinElmer, Optima-8000, and USA). The instrument was calibrated using NIST standards ranging from 2 to 10 ppm. All assays were carried out in triplicate.

2.7 MRSA total membrane lipid extraction

The fatty acid composition of MRSA was determined according to Evans' method (1998). MRSA cultures were treated with **5i** analogue at twice the MIC value. The damaged MRSA culture was collected after 2 hours by centrifugation at 300 rpm for 10 minutes. The bacterial pellet was collected and re-suspended in 2 mL of sterilized water in a 50 mL test tube, and 3.75 mL of methanol/chloroform (2:1, v/v) mixture was added, vortexed and shaken for 2 hours in a rotary shaker. The tubes were centrifuged for 15 minutes at 2500 rpm after the specified time and the supernatant was collected. The extraction was repeated with (4.75 mL × 2) of methanol/chloroform/water (2:1:0.8, v/v) mixture and the supernatants pooled. Finally, 3.8 mL of chloroform was added, followed by an equal volume of water. Vortexed and phase separation was achieved. The lower lipid-containing chloroform fraction was transferred to a glass tube and evaporated with a stream of nitrogen gas. The extract was then treated with a small amount of chloroform, sealed, and stored at 4° C for short-term storage and -20° C for long-term storage.

2.7.1 MRSA membrane damage evaluation by fatty acid profiling

A gas chromatography equipped with a flame ionization detector was used to analyze the fatty acid profile (GC-FID). Fatty acid was trans esterified (obtained after extraction) in a water bath at 50° C for at least 8 hours with 5 mL of the methylation mixture (2:1:1 mixture of methanol, sulfuric acid, and toluene). The formed fatty acid methyl ester (FAME) was extracted by vortex with 3 mL of diethyl ether, and the upper phase was passed through anhydrous sodium sulphate to remove the water. The sample was filtered through a 0.22 µm nylon filter before being stored in an auto sampler vial. Chromatic-Crystal 9000GC with split/split less injector and FID detector was used. Rt-2560 column, 100 m length, 0.25 mm ID, 0.20 µm was used. The following was the chromatographic test condition. The column's initial temperature was 100° C, which was held for 4 minutes, followed by a 3° C/min ramp to 250° C, which was held for 30 minutes. The flow rate of the carrier gas (nitrogen) was 1 mL/min. The retention time of standard FAME peaks was used to identify the fatty acid. The results were processed with built-in software and expressed as a percentage of each fatty acid[30].

2.8 Anti-biofilm activity of 5i analog on sessile MRSA

The anti-biofilm activity of the synthesized analogue **5i** was investigated qualitatively as well as quantitatively[31]. In each well of the microtiter plate, 20 µL of MRSA cell suspension and 180 µL of BHI broth supplemented with glucose were dispensed. Graded concentrations of synthesized analogues were added to these and incubated at 37 °C for 18 hours.

The wells were then washed three times with sterile saline before the cells were fixed for 20 minutes in 150 µL of methanol, air dried, and stained with 0.5% crystal violet for 15 minutes. The wells were completely dried before being washed three times to remove the excess stain. To elute the dye, 150 µL of 95% ethanol was added. In a micro titer plate spectrophotometer, the OD of the eluate was measured at 490 nm. All assays were carried out in triplicate. SEM was used to examine the morphology of the biofilm after it had been fixed with 2.5% glutaraldehyde and mounted on top of an aluminum stub with carbon tape, sputter-coated with gold, and examined[32].

2.9 Effect of compound 5i on MRSA induced coagulation

The anti-coagulation activity of synthesized compound **5i** was investigated by using coagulase positive MRSA and coagulase negative *S.epidermidis* [33]. In Eppendorf tubes, 150 µL of previously reconstituted rabbit plasma in sterile saline water was mixed with 50 µL of different concentrations (25-250g/mL) of **5i** and 50 µL of overnight *S. aureus* culture and incubated at 37 °C for 4 hours. Every hour, anticoagulation activity was monitored and data for clot formation was collected by tilting tubes. Rabbit plasma and rabbit plasma containing *S. aureus* were used as negative and positive controls respectively, and Dabigatran drug was used as a comparison standard.

2.10 Biocompatibility

2.10.1 RBC's hemolysis rate

The compound **5i** was added to freshly drawn sheep blood at various concentrations (0.065, 0.125, 0.25, 0.50, 1.0, 2.0, 5.0, and 10.0 mg/mL), incubated at 37 °C for 30 minutes, and centrifuged at 3000 rpm for 5 minutes. The absorbance of the supernatant was measured at 545 nm[34]. The hemolysis rate (HR) was calculated.

3. Results and Discussions:

3.1. Pharmacophore model, ADME and BBB analysis of synthesized compounds

The synthesized compounds should have both good pharmacological and pharmacokinetic properties to consider as a possible drug candidate. When creating a new molecule intended for therapeutic use, it is crucial to assess its compliance with Lipinski's criteria and to analyze synthesized molecule's adsorption, distribution, metabolism, and excretion (ADME)[35]. According to Lipinski's rule, an oral bioavailability medication can only be in violation of one of the following rules: (1) There can be a maximum of five hydrogen bond donors, and (2) there can be a maximum of ten hydrogen bond acceptors. (3) There must be a molecular weight (MW) of less than 500 D. (4) A partition coefficient (milogP) of octanol and water that is not more than 5. As shown in **Table 1**, the synthesized pyrrole-based carboxamide molecules perfectly met Lipinski's rule. The synthesized molecules can be considered as drug candidates. Contrarily, substances with topological surface area (TPSA) values greater than 140 A^O exhibit lower oral bioavailability[36]. **Table 1** lists the synthesized compound's derived TPSA values. "Pharmacological activity" describes how drugs benefit living organisms. A drug is intended to bind a biological target. The most well-liked proteins, such as receptors, ion channels, and enzymes, are referred to as biological targets. Biological targets are also known as drug targets. The synthesized compounds were given score for their bioactivity based on a number of factors, such as their ability to bind to nuclear receptor ligands and G protein-coupled receptor (GPCR) ligands, modulate ion channels, inhibit kinases and proteases, and inhibit enzymatic activity. The bioactivity rating of the synthetic substances can be determined by the online web application Molinspiration. A molecule is said to be active, when its bioactivity score is >0.0. Called as inactive when the score is less than -5.0. One with a score between -5.0 to 0.0 is called moderately active[37]. The synthesized compounds got outstanding bioactivity score due to the presence of imines, electron donating groups, and withdrawing groups. **Supplementary Table S1** lists the bioactivity scores of the produced drugs. The synthesized compounds exhibited modest activity in nuclear receptor ligand, protease inhibition, and ion channel modulation (**Supplementary Figure S1 and S2**). The synthesized compounds were effective in inhibiting enzyme activity, kinase activity, and G protein-coupled receptor (GPCR) ligand. In **supplementary Figure S1**, the physicochemical fields of synthesized compounds that can pass through the blood brain barrier (BBB) and gastrointestinal absorption (GI) are depicted. The white region of the figure represents the physicochemical field of the molecule that is absorbed by the gastrointestinal system, and the yellow region represents the physicochemical field of the synthesized compounds that can pass through the brain. The formula % Abs = 109 - 0.345 TPSA was used to determine the percentage of absorption of the substances[38]. Except compounds **5c**, **5d**, and **5l** all the other compounds had shown good BBB permeability. Every single synthetic molecule satisfies Lipinski's criteria and possesses the drug-likeness attribute.

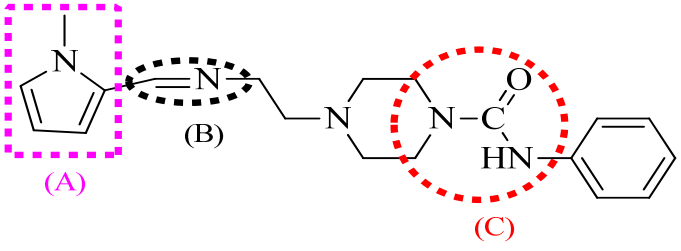

Fig. 2. Pharmaco model of synthesized compounds

Table 1. ADME analysis of synthesized compound 5(a-l

Compound	mi log p	TPSA(A°)	MW <500	n-ON<10	n-OH NH<5	n-rotb	%ABS	Vio<1	BBB
5(a)	3.00	63.73	339.21	3	2	7	87.006	0	Yes
5(b)	3.35	63.73	353.22	3	2	7	87.006	0	Yes
5(c)	3.39	72.96	369.22	4	2	8	83.828	0	No
5(d)	2.7	83.96	355.20	4	3	7	80.003	0	No
5(e)	3.29	63.73	373.17	3	2	7	87.006	0	Yes
5(f)	3.3	63.73	373.17	3	2	7	87.006	0	Yes
5(g)	3.05	63.73	373.17	3	2	7	87.006	0	Yes
5(h)	3.53	63.73	407.13	3	2	7	87.006	0	Yes
5(i)	3.15	63.73	357.43	4	2	7	87.006	0	Yes
5(j)	3.38	63.73	418.33	3	2	7	87.006	0	Yes
5(k)	3.43	63.73	465.33	3	2	7	87.006	0	Yes
5(l)	2.79	109.55	384.13	5	2	8	71.205	0	No

3.2. PASS Biological activity spectrum of synthesized compounds 5a-5l

The PASS software is a free web tool that is used to determine the biological activity spectrum of synthesized compounds. The PASS values of the synthesized compounds were tabulated in **supplementary Table 2**. All the synthesized compounds show the Pa (probable activity) values greater than the Pi (probable inactivity) values, this indicates that the synthesized compounds have the potential to be a drug. The compounds had shown potent values of Pa (probable activity) as an Antineoplastic (lung cancer), antineoplastic, Antineoplastic (brain cancer), Protein kinase inhibitor, Antineoplastic (lymphotic leukemia), Antineoplastic (melanoma), Antineoplastic (multiple myeloma), Anxiolytic, Aurora-c-kinase inhibitor, chemosensitizer. The Pa and Pi values of the compound **5i** is tabulated in **Table 2**. The synthesized compounds exhibit excellent Pa and Pi values, it indicates their potential use for futuristic therapeutic agent.

Table 2. Predicted biological activities of the compound 5i, Pa (probability "to be active"), Pi (probability "to be inactive")

Activity	5i	
	Pa	Pi
Antineoplastic	0.636	0.038
Protein kinase inhibitor	0.158	0.086
Antineoplastic (lymphatic leukemia)	0.188	0.041
Antineoplastic(melanoma)	0.188	0.062
Antineoplastic(multiple myeloma)	0.432	0.017
Anxiolytic	0.215	0.111
Aurora-c-kinase inhibitor	0.248	0.018
Chemo-sensitizer	0.558	0.011

3.3. Molecular docking study

Using Auto Dock 1.5.7, docking studies were undertaken to fit pyrrole compounds bearing carboxamide groups into the active site of the protein 6FTB and 3VMT to understand the mechanism of antibacterial activity. The synthesized molecules were able to access the active region of the proteinoids 6FTB and 3VMT (**Fig. 3**), confirmed that they got a high docking score and strong interactions such as hydrogen, Van derwaals, and hydrophobic with potential amino acid residues. The docking results of the synthesized compounds are tabulated in the **supplementary Table 3 and 4**. Among the 12 synthesized compounds, compound **5i** had shown potential binding energy of -9.11. The N-H group of the compound **5i** formed one conventional hydrogen bond with M A: 0E301, due to this interactions compound **5i** exhibited good binding energy. The phenyl and piperazine ring formed one pi-alkyl and alkyl interaction with ARG A: 148 and one Van der waals interaction with EDO A: 310. In this study, the compound **5i** had shown good docking score compared to other analogues and also this theoretical data strongly correlated to our experimental results.

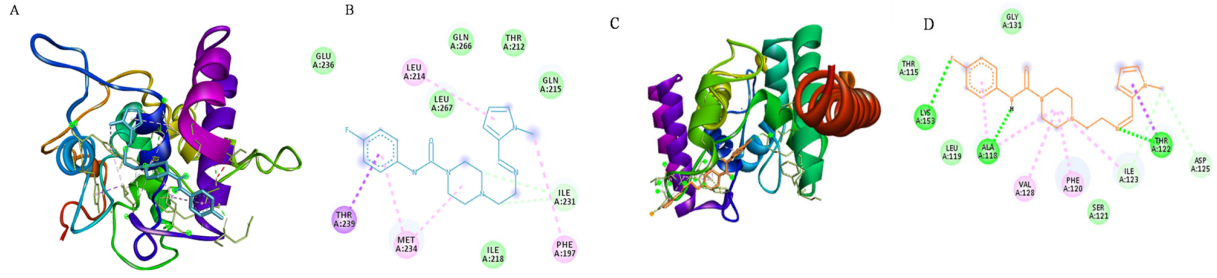

Fig. 3. Molecular docking proof for **6FTB** (A&B), **3VMT**(C&D) proteins of MRSA intern best pose at active sites of targets by **5i**.

3.4. Synthesis and characterization

As illustrated in **Fig. 1**, pyrrole-based carboxamide derivatives of (Z)-4-(2-((1-methyl-1H-pyrrol-2-yl) methylene) amino) ethyl)-N-phenylpiperazine-1-carboxamide were synthesized in the present study. The structure of the synthesized compounds is tabulated in **supplementary table S5** and spectral data are provided in **supplementary file 1.1**. Spectral investigations were used to determine the structure of synthesized compounds. It was a multi-step synthesis involving 1-methyl-1H-pyrrole-2-carbaldehyde (**1**) and 2-(piperazin-1-yl) ethane. -1-amine (**2**) were used to synthesize the compound (Z) N-(2-(piperazin-1-yl) ethyl)methanimine -1-(1-methyl-1H-pyrrol-2-yl)-N-(2-(piperazin-1-yl)ethyl)methanimine (**3**). We also examined compound **3** with a different spectral approach. FT-IR spectrum of compound **3** shown bands at 1260 cm^{-1} indicated the presence of a NH group, whereas the peak at 1620 cm^{-1} indicated the presence of C=N(imine) moieties. The molecular ion peak (m/z) of compound **3** is 220.17, whereas ^{1}H-NMR spectrum indicated a singlet peak at 3.91 ppm, showing the presence of N-CH_3 proton, and singlet peak at 8.28 ppm indicating the presence of imine proton. These spectra confirm the structure of compound **3**. The series of analogues **5(a-l)** were synthesized using (Z)-1-(1-methyl-1H-pyrrol-2-yl)-N-(2-(piperazin-1-yl) ethyl) methanimine and substituted isocyanatobenzene scheme as shown in figure 1. Evaluation of synthesized series of analogues **5 (a-l)** by various spectral methods, FT-IR spectra of all compounds recorded within range of 4000-400 cm^{-1}. The C=N group has a strong absorption band at 1680 cm^{-1}, the carboxamide (CONH) stretching band was shown at 2250 cm^{-1}. These findings confirmed that the analogues **5(a-l)** have excellent spectral data validation. $CDCl_3$ was used to report the synthesized compounds' distinctive resonance peak in ^{1}H-NMR and ^{13}C NMR. The resonance was allocated to them based on their peak multiplicity and integration. The newly synthesized compounds showed excellent agreement with the integration spectra. The ^{1}H-NMR spectra of compound **5i** exhibited a singlet peak at 9.80 ppm, which could be assigned to the CH=N proton, and a singlet peak at 5.24 ppm, and ascribed to the N-CH_3proton. The pyrrole protons were indicated by two doublet peaks at 8.21 and 7.22 ppm. The piperazine protons were shown by a doublet peak at 3.39 and 3.82 ppm. Aromatic protons also produce a doublet peak to appear between 6 to 7 ppm. The compounds **(5a-5l)** exhibited a single peak between 3 to 4 ppm that indicated the presence of CH_3 attach to the pyrrole ring. The ^{13}C NMR spectra for **5a-5l** indicated that the groups were in the range of 40-180 ppm. The saturated carbon atoms show peaks below 100ppm and unsaturated carbon atoms show peaks in the range 100-160ppm. The observed molecular ion peak value in the mass spectra of compounds **5a-51** was in good agreement with the molecular formula of produced compounds (**Supplementary Figure S4 –S13**). The molecular ion peak for the compound **5i** was found at m/z 357.43, which matched with the molecular formula $C_{19}H_{24}FN_5O$.

3.5. Antibacterial activity

Methicillin-resistant *S. aureus* (MRSA) is already widespread in clinics and communities, and vancomycin-resistant strains have recently emerged, making treatment more challenging[39]. If we have a better understanding of how MRSA interacts with the host, it will be helpful to create novel therapeutic approaches in the light of the rising antibiotic resistance. The antibacterial potency of pyrrole coupled carboxamide derivatives **5(a-l)** evaluated by resazurin and disc diffusion method. The different graded concentration of **5(a-l)** (10-100 µg/mL) was used to assess the minimum inhibitory concentration against bio-hazardous MRSA culture and data is presented in **Table 3**. The pyrrole coupled carbothioamide derivative **5i** showed an excellent antibacterial action compared to standard antibiotic streptomycin (16.60±0.04mm Zone of inhibition (ZOI)) at 10 µg/disc against MRSA in a dose-dependent manner (20, 25, 30, 35, 40 & 45 µg/mL) with ZOI of 17.30±0.05, 20.10±0.06, 22.60±0.08, 24.80±0.09, 26.20±0.06, and 29.30±0.09 in mm correspondingly **(Fig. 4A and 4B)**.Among all the derivatives, **5i** analog showed higher antibacterial activity when compared to **5e, 5f** and **5j** due to the electron-donating group present in the phenyl ring.

Table 3. Antibacterial activity of the synthesized pyrrole-coupled carboxamide derivatives 5(a-l) against methicillin-resistant *Staphylococcus aureus* (MRSA).

Compound name	MIC in µg/mL
5a	42±0.50
5b	50±0.60
5c	52±0.30
5d	42±0.40
5e	34±0.50
5f	38±0.20
5g	42±0.60
5h	50±0.60
5i	16±0.30
5j	38±0.40
5k	53±0.40
5l	51±0.50
Streptomycin	10

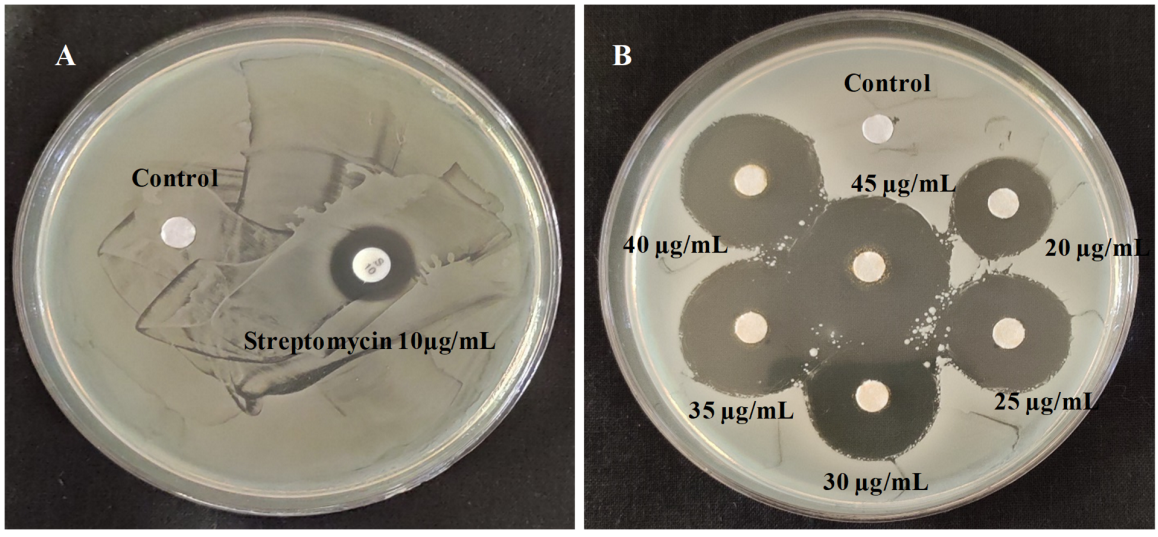

Fig. 4. Antimicrobial activity of **5i** against MRSA. **(A)** MRSA tested with standard drug Streptomycin 10µg/disc (16.10±0.06) ZOI in mm. **(B) 5i** with different concentration ranging from 20, 25, 30, 35, 40 & 45 µg/mL (17.30±0.05, 20.10±0.06, 22.60±0.08, 24.80±0.09, 26.20±0.06, and 29.30±0.09 ZOI in mm respectively).

3.6. Membrane damage study

3.6.1. MRSA membrane cell damage by SEM, cellular leakage, and potassium efflux

Studying the membrane deterioration of MRSA bacterial cells helped to further confirm the antibacterial activity of **5i**. Overnight suspended MRSA bacterial cells were treated with twice the MIC of **5i** and kept an untreated culture as a control. Comparing the SEM of MRSA cell surface of untreated control and the treated bacterial cell surface revealed considerable membrane alterations such as holes, mis-shaped membranes, and breaks **(Fig. 5A and Fig. 5B)**. Further evidence for MRSA's cell membrane destruction was approached from measurement of potassium efflux variation and DNA leakage after cell injury. According to the revealed results, an increasing dose of **5i** caused an increase in the leakage of cellular content and potassium content in the solution. This had shown clearly that MRSA's cell membrane being damaged **(Fig. 6A & 6B)**.

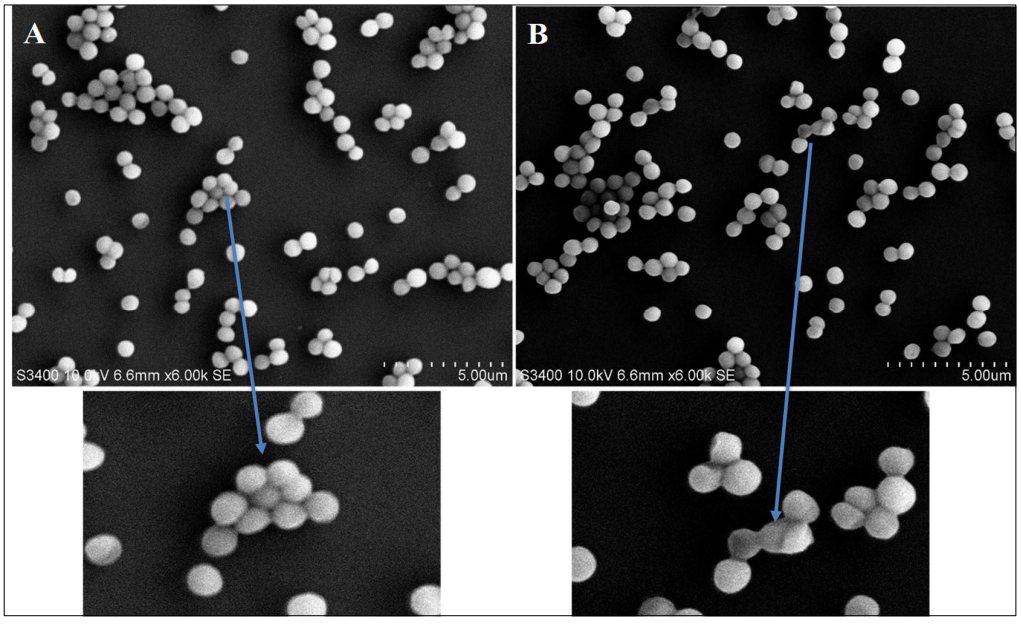

Fig. 5. The MRSA cell membrane damage. **A**. SEM images of untreated MRSA cell surfaces. and **B**. the pyrrole-coupled carboxamide derivative of **5i** treated SEM images shows misshaped bacterial cell surfaces.

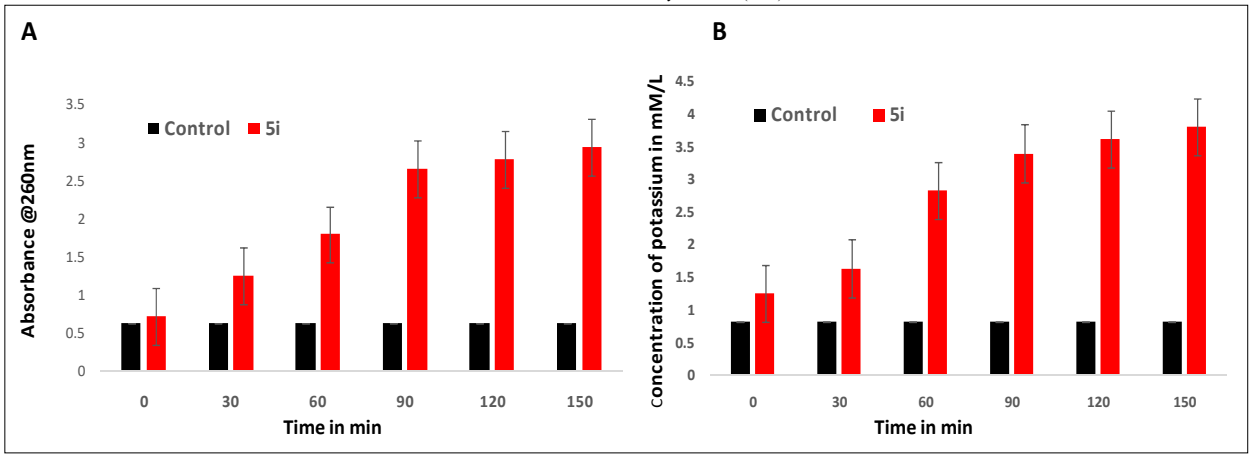

Fig. 6. A. MRSA cell membrane damage assay validated by cellular content (DNA) leakage and **B**. Measurement of potassium content in suspension after treated with **5i**.

3.7. Study of MRSA bacterial membrane destruction by fatty acid profile

Water, metal ions, drug and other factors all affect the balance between rigidity and fluidity in bacterial membranes, but the lipid packing within the membrane which is controlled by the structure and makeup of phospholipid fatty acids is the main driver of this equilibrium. Bacterial membranes in the case of MRSA are mostly made up of straight-chain and branched-chain saturated fatty acids. Branched-chain iso or anti-iso methyl species support a more fluid membrane structure, whereas straight-chain fatty acids form a bilayer with limited permeability qualities by packing together. The ability of compound **5i** to kill bacteria is affected by the alteration of fatty acid composition of the membrane. We hypothesized that modifications to membrane, especially those that altered membrane polarity, may result in the bactericidal effect. Based on this hypothesis, we examined the MRSA fatty acid profile of the growing stage, and of the treated one with double the MIC value compound **5i**. The obtained data were used to help explain the bactericidal activity of compound **5i**. It was related to the kind of fatty acids that make up bacterial membranes (**Fig. 7A, Fig. B & Fig. C**). The revealed data significantly indicated alteration in fatty acid profile of MRSA. The Methyl erucate (C22:1[cis-13]) was the major fatty acid peak which was found to be 49.98% in the controlled MRSA culture, and it was reduced to 10.82% after treatment with compound **5i** (**supplementary Table S6-S8**).

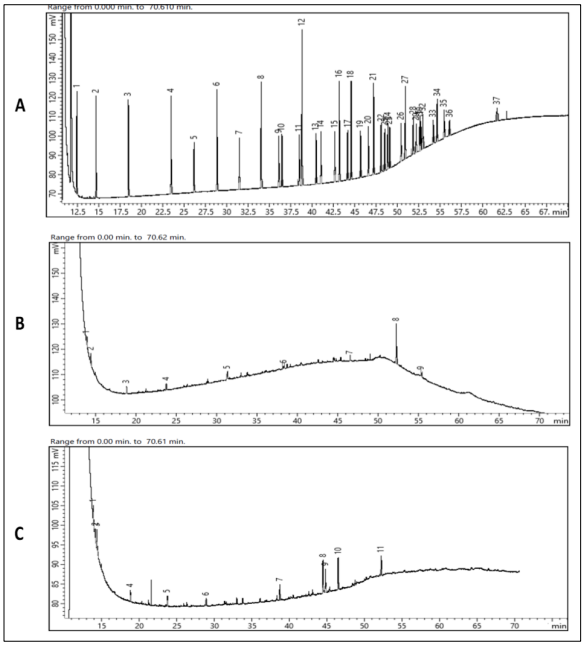

Fig. 7. Chromatogram of fatty acid profile. **A.** 37 standard fatty acid profile mixture, **B.** Control MRSA bacterial culture fatty acid profile pattern and **C.** MRSA bacterial fatty acid profile after treated with **5i** analog.

3.8. The anti-coagulase activity of compound 5i

MRSA is a human communal bacterium that can cause a wide range of diseases, from invasive illnesses like pneumonia, septicemia, and endocarditis to skin and soft tissue infections. In addition to producing several proteins that bind to fibrinogen and encourage clumping, MRSA is unique ability to cause blood to clot. It has been demonstrated that the pathogenicity and immune evasion of MRSA depend critically on the formation of clumps, which are enormous, tightly packed groupings of cells held together by fibrin. Cells can avoid phagocytosis and immune system recognition because of a fibrin layer that acts as a barrier and the size of the clumps. Additionally, as disorders like soft tissue abscesses and endocarditis involve compact cell clusters embedded in host matrix proteins, clumping may be a critical early step in the development of these conditions. To address inhibition of anticoagulation of fibrinogen, an anti-coagulation test was conducted using rabbit plasma to compare the effectiveness of compound **5i** in preventing coagulation against the MRSA coagulase to that of the widely used anti-coagulant medication Dabigatran (Pradaxa). In conclusion, at a dosage of 50µg /mL, compound **5i** demonstrated prevention of coagulation by preventing the conversion of soluble fibrinogen to insoluble fibrin (creamy white clot). The outcome was verified using the widely used standard drug, Dabigatran, which at a modest dose of 10 µg/mL efficiently prevented the formation of coagulation in rabbit plasma (**Fig. 8**).

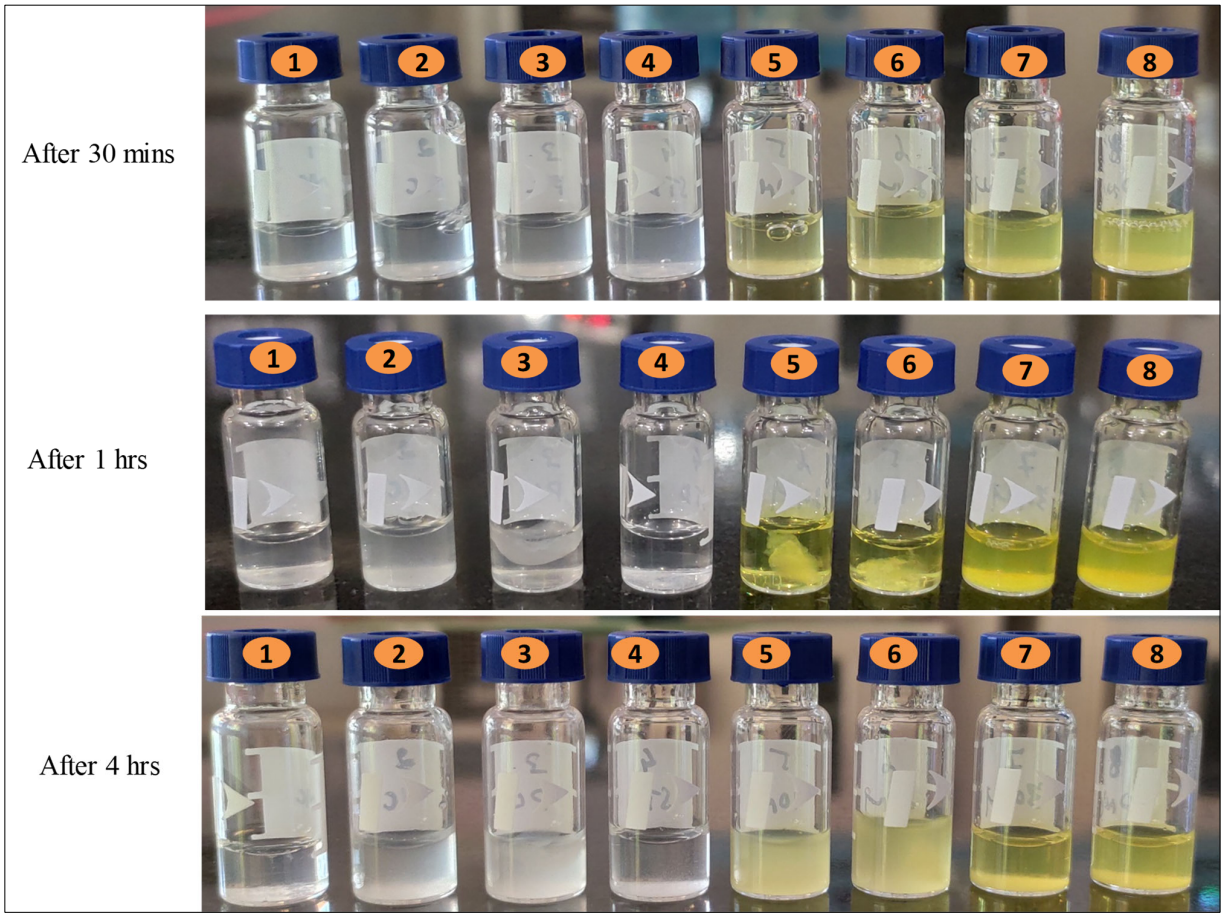

Fig. 8. The images symbolize the potency of anti-coagulation activity of **5i**. Vial 1-are reagent control (only rabbit plasma), Vial 2-are rabbit plasma mixed with 50µL of *S. epidermises* culture as a negative coagulase reaction, Vial 3-are rabbit plasma with MRSA culture, Vial 4-are rabbit plasma mixed with MRSA culture and 10 µg/mL standard drug Dabigatran. Vial 5 to 8 are rabbit plasma and MRSA culture with different concentrations of compound **5i**. All the glass vials were incubated at 37ºC for up to 4 hrs. The images were taken after 30 min, 1 hr and 4 hrs of incubation. This image shows no clot formation in the reagent, negative control. Clot formation in the positive control (untreated) and clot inhibition in the Dabigatran drug at 10µg/mL. The compound **5i treated** sample vials show that it inhibited the fibrin formation at 50 µg/mL.

3.9. Anti-biofilm activity of 5i against sessile MRSA

MRSA bacteria have typically been cultivated as either a biofilm or as free-floating planktonic cells. Although the word "biofilm" is roughly used in the literature, it typically refers to a multilayered cellular population adhered to a surface. These cells have heightened resistance to antibiotics and are embedded in an extracellular matrix made of various combinations of proteins, DNA, and secreted polysaccharides[40]. There is no doubt that biofilm formation contributes to some *staphylococcal* infections, such as the colonization of indwelling devices like catheters, artificial joints, and pacemakers[41].

In MRSA biofilms, cells have been embedded in an extracellular polymeric matrix and form aggregates that are attached to an abiotic or biotic surface or that are non-attached are known as biofilms (free-floating aggregates). In this environment, the metabolism, gene transcription, and protein expression between planktonic cells and cells in biofilms show striking variations. Strong biofilms created by MRSA can cause serious infections that are resistant to antibiotics, most commonly in diabetic patients' chronic skin ulcers and fresh burn wounds. The revealed data showed positive control have matte biofilm grown on the micro triter plate compared to negative control. In this context, the pyrrole-coupled carboxamide derivative **5i**, strongly inhibited the adherence of MRSA bacterium on the surface. At the concentration 200µg/mL, compound **5i** completely inhibited the MRSA biofilm formation (**Fig. 9 A & B**).

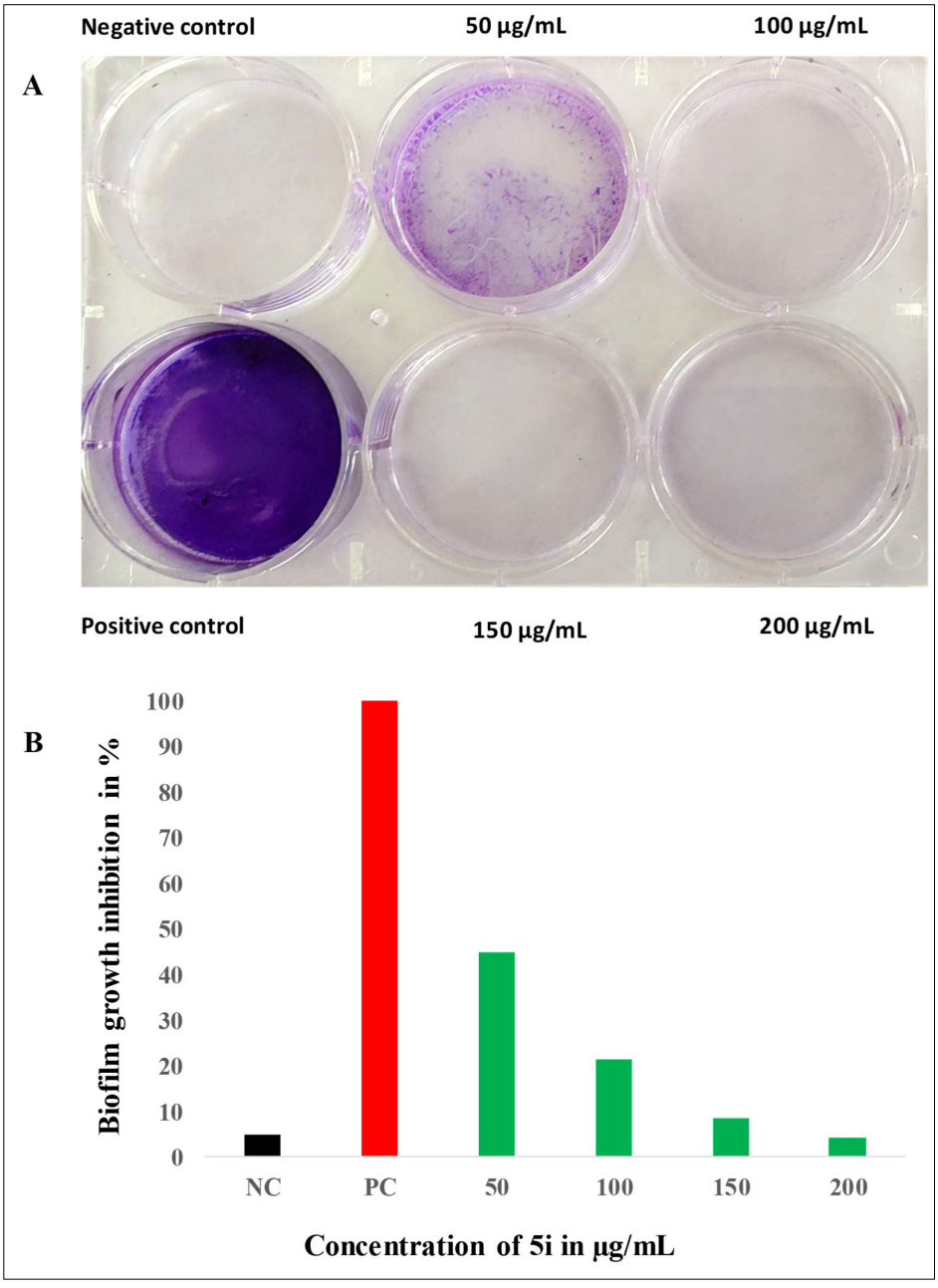

Fig. 9. Anti-biofilm activity of **5i**. **A.** Picture represents the qualitative anti-biofilm activity of crystal violet dye method and **B.** Quantitative anti-biofilm inhibition.

3.10 Biocompatibility study

The blood coagulation assay is one of the most often used techniques for figuring out whether a new medicine or biomaterial is hem compatible. When soluble plasma proteins are activated in response to vascular injury, blood coagulation

is a local cascade process that results in the creation of a fibrin clot. Coagulation may result from exposure to chemicals originating from wounded tissue or surface-mediated processes (intrinsic route) (extrinsic pathway).

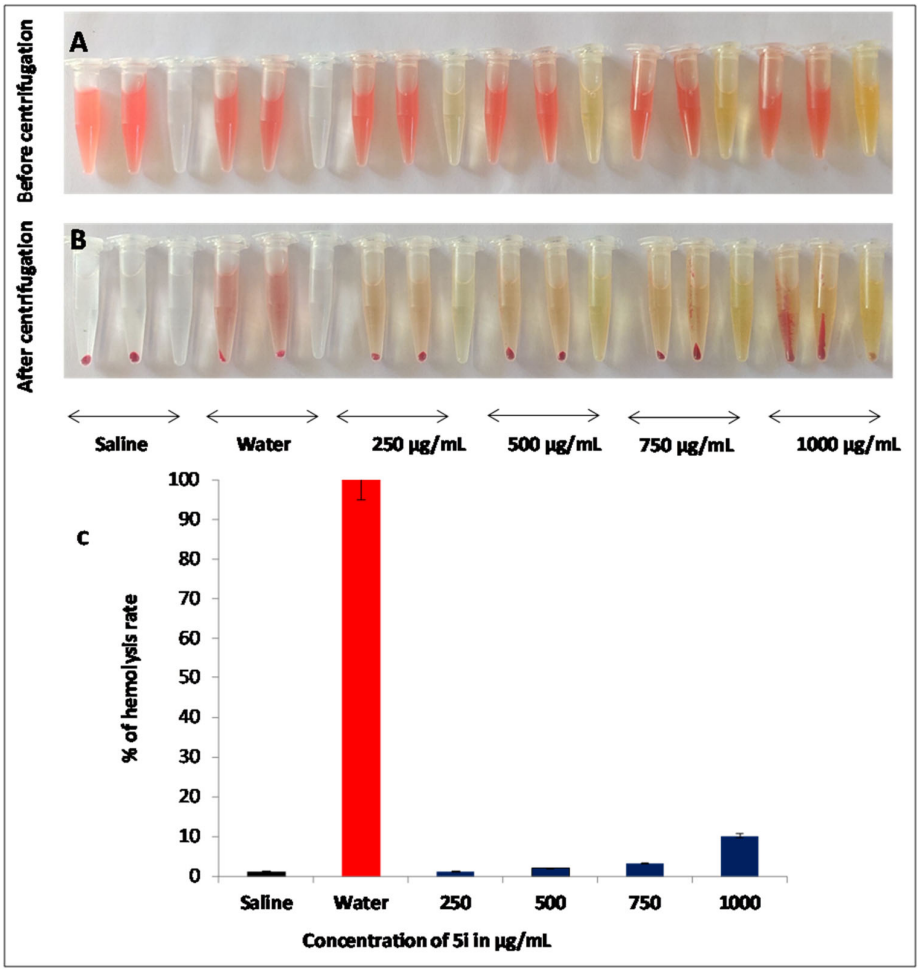

Fig. 10. The blood biocompatibility assay. Images **A, B.** show the before and after centrifugation of effendorf. Tubes. RBC Sediment formation at different concentration of compound **5i** along with saline and water control image. **C.** Shows the % of hemolysis rate.

The two processes come together to create a single pathway that leads to the formation of a clot. These two coagulation pathways are often evaluated using the prothrombin time (PT) and activated partial thromboplastin time (APTT) assays. Bio-compatibility in this context refers to the measurement of blood's cellular and plasma components. Red blood cells (RBCs) are typically hemolyzed to assess hematology, which is regarded as a quick and accurate method for evaluating blood biocompatibility[42]. To establish the safety of the reaction of the synthesized **5i** analogue in the blood stream, it was required to evaluate the biocompatibility of RBCs. Up to values of 750 µg/mL, it was determined that compound **5i** had no effect on the erythrocyte membrane. Typically, some drugs result in an osmotic pressure imbalance in the blood stream, which causes RBCs to lyse out their hemoglobin content. The **5i** analogue addressed the compatibility in this case without altering the RBCs in the biological domain due to its outstanding blood biocompatibility and potent anti-staphylococcal capability (**Figure 10A, B, & C**).

3.11 Toxic effect of analog 5i

The real issue arises when time and money are spent researching compounds that have toxicity issues and must ultimately be dropped from further study. Multiple approaches are used to evaluate toxicity and safety throughout the discovery and development of new medications. Years of research and hundreds of millions of dollars could be wasted if harmful substances are not eliminated in the early stages of research. The MTT assay was used to assess the cytotoxicity of the putative **5i** drug against the 3T3-L1 cell lines and evaluate whether it had an anti-proliferative effect. In this assay, we opted compound 5i in the cytotoxicity assay because it was found to be a potent contender to MRSA. The synthesized **5i** derivative has an IC_{50} value of 286.70 µg/mL in contrast to the reference drug Doxorubicin 20.45 µg/mL, in accordance with the information which is presently available (**Fig. 11**).

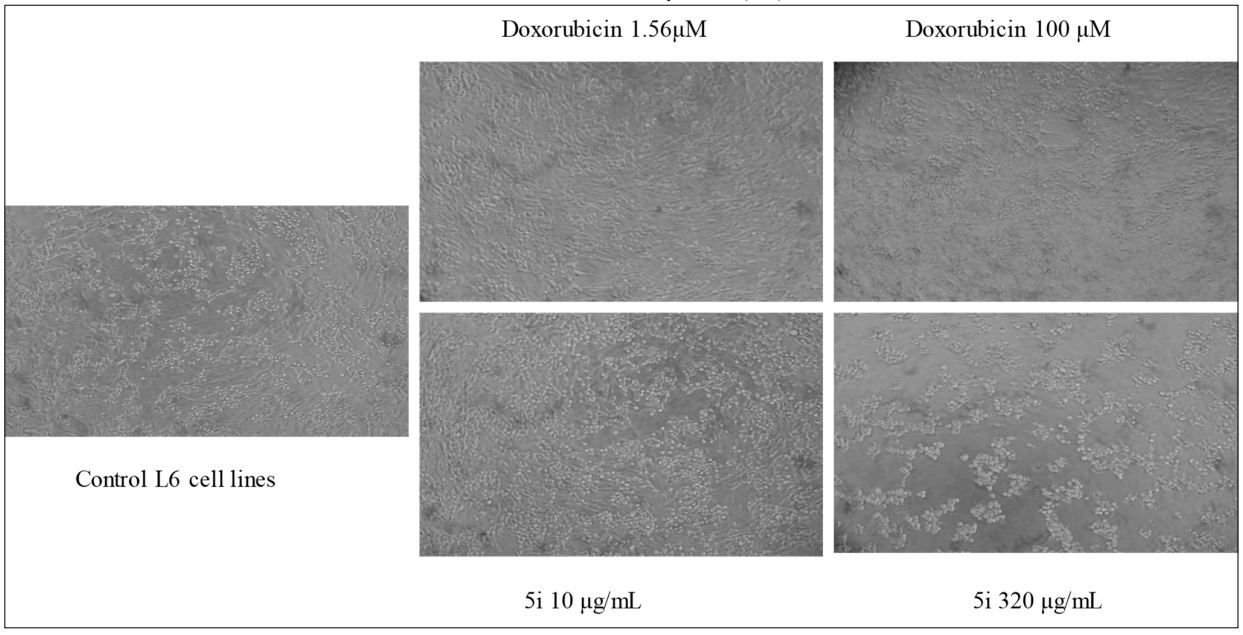

Fig. 11. % inhibition of L6 cell line cells with different concentration of Doxorubicin and 5i

4. Conclusion

In this investigation, we designed and synthesized the various pyrrole-coupled carboxamide derivatives 5(a-l) as promising antibacterial agents and particularly against MD-MRSA. Several different methodologies were used to amply characterize each derivative. The nature of drug-likeness was thoroughly examined using Pharmacophore, ADME, and BBB. Utilizing *in-vitro* methods, such as measuring DNA leakage, potassium efflux, and fatty acid profile of MRSA bacterial cell membrane disruption, the antibacterial potency of the synthesized drug was demonstrated. Theoretically, the anti-MRSA activity was again validated by an *in silico* docking study on the MRSA protein 6FTB, which showed a good docking score and binding energy. The compound **5i** had shown good biocompatibility and was less harmful to normal cell lines. We reached the conclusion based on the revealed data, further modifying of the compound **5i** will have significant therapeutic uses for bacteremia, endocarditis, sepsis, and scaling skin infections associated with MRSA.

Author Contribution

BAV conducted the experiment, lead the entire project, and performed the computational studies. GT and SK: Reviewed and improved the quality of the manuscript by suggestions, and supervisions. All authors have critically reviewed and approved the final draft and are responsible for the content and similarity index of the manuscript.

Funding

This research did not receive any specific grant from funding agencies in the public, commercial, or not for profit sectors.

Acknowledgments

We thank Skanda Life Sciences Pvt Ltd., Bengaluru, Karnataka, for carrying out and providing the cytotoxicity data.

References

1. Alanis A. J. **(2005)** Resistance to antibiotics: are we in the post-antibiotic era? *Arch. Med. Res.*, 36(6) 697-705.
2. Nobili S., Lippi D., Witort E., Donnini M., Bausi L., Mini, E., and Capaccioli S. **(2009)** Natural compounds for cancer treatment and prevention. *Pharmacol. Res.*, 59(6) 365-378.
3. Harrus S., and Baneth G. **(2005)** Drivers for the emergence and re-emergence of vector-borne protozoal and bacterial diseases. *Int. J. Parasitol.,* 35(11-12) 1309-1318.
4. Chandrasekaran B., Abed S. N., Al-Attraqchi O., Kuche K., and Tekade R. K. **(2018)** Computer-aided prediction of pharmacokinetic (ADMET) properties. *In Dosage form design parameters.* 731-755.
5. Gershell L. J., and Atkins J. H. **(2003)** A brief history of novel drug discovery technologies. *Nat. Rev. Drug Discov.,* 2(4) 321-327.

6. Chandrasekaran N., Selvakumar K., Premkumar V., Muthusamy S., Senthil Kumar S. M., and Thangamuthu R. **(2018)** Dual heteroatom-doped carbon monoliths derived from catalyst-free preparation of porous polyisocyanurate for oxygen reduction reaction. *ACS Sustain. Chem. Eng.*, 6(7) 9094-9103.
7. Cho S. H., Kim J. Y., Kwak J., and Chang S. **(2011)** Recent advances in the transition metal-catalyzed twofold oxidative C–H bond activation strategy for C–C and C–N bond formation. *Chem. Soc. Rev.*, 40(10) 5068-5083.
8. Nazeri M. T., and Shaabani A. **(2021)** Synthesis of polysubstituted pyrroles via isocyanide-based multicomponent reactions as an efficient synthesis tool. *New J. Chem.*, 45(47) 21967-22011.
9. Senge M. O., MacGowan S. A., and O'Brien J. M. **(2015)** Conformational control of cofactors in nature–the influence of protein-induced macrocycle distortion on the biological function of tetrapyrroles. *Chem comm.*, 51(96) 17031-17063.
10. Prasad H. N., Ananda A. P., Lohith T. N., Prabhuprasad P., Jayanth H. S., Krishnamurthy N. B., and Mallu P. **(2022)** Design, synthesis, molecular docking and DFT computational insight on the structure of Piperazine sulfynol derivatives as a new antibacterial contender against superbugs MRSA. *J. Mol Struct.,* 1247 131333.
11. Hwu J. R., Roy A., Panja A., Huang W. C., Hu Y. C., Tan K. T., and Tsay S. C. **(2020)** Domino Reaction for the Synthesis of Polysubstituted Pyrroles and Lamellarin R. *J. Org. Chem.*, 85(15) 9835-9843.
12. Singh N., Singh S., Kohli S., Singh A., Asiki H., Rathee G., and Anderson E. A. **(2021)** Recent progress in the total synthesis of pyrrole-containing natural products. *Org. Chem. Front.*, 8(19) 5550-5573.
13. Ahmad S., Alam O., Naim M. J., Shaquiquzzaman M., Alam M. M., and Iqbal M. **(2018)** Pyrrole: An insight into recent pharmacological advances with structure activity relationship. *Eur. J. Med. Chem.,* 157 527-561.
14.Khandelwal S., Tailor Y. K., Rushell E., and Kumar M. **(2020)** Use of sustainable organic transformations in the construction of heterocyclic scaffolds. *In Green App in Med Chem for Sust Drug Des* .245-352.
15. Slobodníková L., Fialová S., Rendeková K., Kováč J., and Mučaji P. **(2016)** Antibiofilm activity of plant polyphenols. *Molecules.,* 21(12) 1717.
16. Prasad H., Ananda A., Mukarambi A., Gaonkar N., Sumathi S., Spoorthy H., and Mallu P. **(2023)** Design, synthesis, and anti-bacterial activities of piperazine based phthalimide derivatives against superbug-Methicillin-Resistant Staphylococcus aureus. *Curr. Chem.*, 12(1) 65-78.
17. Oblak M., Kotnik M., &Solmajer T. **(2007)** Discovery and development of ATPase inhibitors of DNA gyrase as antibacterial agents. *Curr. Med. Chem.*, 14(19) 2033-2047.
18. Oh J. H., Lee T. J., Park J. W., and Kwon T. K. **(2008)** Withaferin A inhibits iNOS expression and nitric oxide production by Akt inactivation and down-regulating LPS-induced activity of NF-κB in RAW 264.7 cells. *Eur. J. Pharmacol.*, 599(1-3) 11-17.
19. Huang Y., Dong G., Li H., Liu N., Zhang W., and Sheng C. **(2018)** Discovery of janus kinase 2 (JAK2) and histone deacetylase (HDAC) dual inhibitors as a novel strategy for the combinational treatment of leukemia and invasive fungal infections. *J. Med. Chem.*, 61(14) 6056-6074.
20. Huizing M. T., Misser V. S., Pieters R. C., ten BokkelHuinink W. W., Veenhof C. H. N., Vermorken J. B., and Beijnen J. H. **(1995)** Taxanes: a new class of antitumor agents. *Cancer Invest.*, 13(4) 1-404.
21.Gill R. K., Rawal R. K., and Bariwal J. **(2015)** Recent advances in the chemistry and biology of benzothiazoles. *Arch. Pharm.*, 348(3) 155-178.
22. Seelig A., Gottschlich R., and Devant R. M. **(1994)** A method to determine the ability of drugs to diffuse through the blood-brain barrier. *Proc. Natl. Acad. Sci.*, 91(1) 68-72.
23.Tatar E., Şenkardeş S., Sellitepe H. E., Küçükgüzel Ş. G., Karaoğlu Ş. A., Bozdeveci A., and Küçükgüzel İ. **(2016)** Synthesis, and prediction of molecular properties and antimicrobial activity of some acylhydrazones derived from $ N $-(arylsulfonyl) methionine. *Turk. J. Chem.*, 40(3) 510-534.
24.Hossen M. A., Reza A. A., Ahmed A. A., Islam M. K., Jahan I., Hossain R., and Rahman M. A. **(2021)** Pretreatment of Blumealacera leaves ameliorate acute ulcer and oxidative stress in ethanol-induced Long-Evan rat: A combined experimental and chemico-biological interaction. *Biomed. Pharmacother.*, 135 111211.
25. Kandhare A. D., Bodhankar S. L., Singh V., Mohan V., and Thakurdesai P. A. **(2013)** Anti-asthmatic effects of type-A procyanidine polyphenols from cinnamon bark in ovalbumin-induced airway hyperresponsiveness in laboratory animals. *Biomed. Aging Pathol.*, 3(1) 23-30.
26.Roman M., Roman D. L., Ostafe V., Ciorsac A., and Isvoran A. **(2018)** Computational assessment of pharmacokinetics and biological effects of some anabolic and androgen steroids. *Pharm. Res.,* 35 1-25.
27. Prasad H. S. N., Gaonkar N. P., Ananda A. P., Mukarambi A., Kumar G. C., Lohith T. N., and Beeregowda N. **(2022)** Antibacterial Property of Schiff-based Piperazine against MRSA: Design, Synthesis, Molecular Docking, and DFT Computational Studies. *Lett. Appl. NanoBioScience.,* 2 54.
28.Kamdem D. P., Shen Z., Nabinejad O., and Shu Z. **(2019)** Development of biodegradable composite chitosan-based films incorporated with xylan and carvacrol for food packaging application. *Food Packag. Shelf Life.*, 21 100344.
29.Zhang Y., Zeng X., Wang H., Fan R., Hu Y., Hu X., and Li J. **(2021)** Dasatinib self-assembled nanoparticles decorated with hyaluronic acid for targeted treatment of tumors to overcome multidrug resistance. *Drug Deliv.*, 28(1) 670-679.
30.Yu Y., Wang G., Yin X., Ge C., and Liao G. **(2021)** Effects of different cooking methods on free fatty acid profile, water-soluble compounds and flavor compounds in Chinese Piao chicken meat. *Food Res Int.*, 149 110696.
31. Mohanta Y. K., Biswas K., Jena S. K., Hashem A., Abd_Allah E. F., and Mohanta T. K. **(2020)** Anti-biofilm and antibacterial activities of silver nanoparticles synthesized by the reducing activity of phytoconstituents present in the Indian medicinal plants. *Front Microbiol.*, 11 1143.

32.Witcomb M. J. **(1981)** The suitability of various adhesives as mounting media for scanning electron microscopy: I. Epoxies, sprays and tapes. *J. Microsc.,* 121(3) 289-308.
33.Bocian A., and Hus K. K. **(2020)** Antibacterial properties of snake venom components. *Chem. Pap.*, 74 407-419.
34. Chen D., Tang Q., Li X., Zhou X., Zang J., Xue W. Q., and Guo C. Q. **(2012)** Biocompatibility of magnetic Fe3O4 nanoparticles and their cytotoxic effect on MCF-7 cells. *Int J Nanomedicine.,*4973-4982.
35. Sowmya M., Puttaswamy A A., Shivabasappa H., Prasad N., Geetha N., Girija S., & Venkatachalam P. **(2022).** Biogenic Synthesis of *Alternanthera sessilis* Titanium Dioxide Nanoparticles (AS@ TiO2NP's): A Potential Contender against Perilous Pathogens and Catalytic Degradation of Organic Dyes. *Biointerface Res. Appl. Chem.,* 13(5), 462.
36. Alafeefy A. M., Bakht M. A., Ganaie M. A., Ansarie M. N., El-Sayed N. N., and Awaad A. S. **(2015)** Synthesis, analgesic, anti-inflammatory and anti-ulcerogenic activities of certain novel Schiff's bases as fenamate isosteres. *Bioorg. Med. Chem. Lett.*, 25(2) 179-183.
37. Kokubo T., Kim H. M., Kawashita M., and Nakamura T. **(2004)** REVIEW Bioactive metals: preparation and properties. *J. Mater Sci Mater Med.*, 15 99-107.
38.Laursen J. B., and Nielsen J. **(2004)** Phenazine natural products: biosynthesis, synthetic analogues, and biological activity. *Chem. Rev.*, 104(3) 1663-1686.
39.Weber S. G., Huang S. S., Oriola S., Huskins W. C., Noskin G. A., Harriman K., and Karchmer T. B. **(2007)** Legislative mandates for use of active surveillance cultures to screen for methicillin-resistant Staphylococcus aureus and vancomycin-resistant enterococci: position statement from the Joint SHEA and APIC Task Force. *Infect Control Hosp Epidemiol.*, 28(3) 249-260.
40.Borlee B. R., Goldman A. D., Murakami K., Samudrala R., Wozniak D. J., and Parsek M. R. **(2010)** Pseudomonas aeruginosa uses a cyclic-di-GMP-regulated adhesin to reinforce the biofilm extracellular matrix. *Mol. Microbiol.*, 75(4) 827-842.
41.Rohde H., Frankenberger S., Zähringer U., and Mack D. **(2010)** Structure, function and contribution of polysaccharide intercellular adhesin (PIA) to Staphylococcus epidermidis biofilm formation and pathogenesis of biomaterial-associated infections. *Eur. J. Cell Biol*, 89(1) 103-111.
42. Prasad H. N., Ananda A. P., Sumathi S., Swathi K., Rakesh K. J., Jayanth H. S., and Mallu P**. (2022)** Piperazine selenium nanoparticle (Pipe@ SeNP's): A futuristic anticancer contender against MDA-MB-231 cancer cell line. *J. Mol Struct.*, 1268 133683.